

AD-A149 704

CIRCULATION AND INTERNAL WAVES IN A COLD GULF STREAM
WAVES(U) WASHINGTON UNIV SEATTLE APPLIED PHYSICS LAB
T B SANFORD OCT 84 N00014-84-C-0187

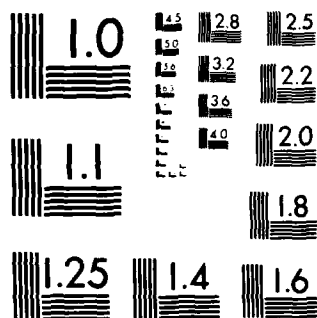
1/1

UNCLASSIFIED

F/G 8/3

NL

										END			
										FORM			
										DT			



MICROCOPY RESOLUTION TEST CHART
NATIONAL BUREAU OF STANDARDS 1963-A

12

AD-A149 704

Final Report on ONR Contract N00014-84-C-0187

on the Circulation and Internal Waves

in a Cold Gulf Stream Ring

Thomas B. Sanford

Applied Physics Laboratory

and School of Oceanography

University of Washington

Seattle, WA 98105

DTIC
ELECTE
JAN 30 1985
S B D

October 1984

1. Introduction

Under this program an existing salt-bridge GEK was refurbished and used extensively in the Florida Current and Gulf Stream. The purposes of these measurements were to measure the ambient electric field in the ocean and to determine from a moving vessel the voltage differences across the Current and Stream. The experiment was conducted as part of a joint ONR-NOAA sponsored cruise on the USNS Lynch.

The GEK is a device to measure the voltage between two points at or near the sea surface at separations of about 16 m. These voltages are converted to the components of the quantity $v - \frac{\vec{v}}{v}$ normal to the track of the ship by dividing the voltages by 16 m and the local vertical component of the earth's magnetic field. The velocity determined by the GEK is the difference between the surface velocity (normal to the ship's heading), denoted at v , and the normal component of the vertical-

DTIC FILE COPY

DISTRIBUTION STATEMENT A

Approved for public release
Distribution Unlimited

84 11 09 012

ly averaged velocity, \bar{v} . It is possible to separate the two contributions using the independent information from LORAN-C navigation.

The velocity component of the ocean normal to the ship's heading was determined by tracking several LORAN-C stations using a precise receiver, Internav LC404, in a range-range mode. The accuracy of the LORAN system developed for this work is estimated to be about 1 cm/s over 5 minute intervals. The vessel's gyrocompass was used to determine heading. The LC404 was leased for the cruise from the manufacturer.

2. The Instrumentation

The GEK/LORAN system as configured for the Lynch cruise is shown in Fig. 1. The radio navigation information from SATNAV and LORAN-C is logged by the project computer along with ship's heading. The GEK is controlled by a separate deck unit that transfers the data to the computer.

The GEK underwent extensive improvement and changes. Fig. 2 is a block diagram of the GEK and controller. The GEK consists of solenoids for actuating the valves that modulate the conductances of the paths from the electrodes to the tube ends. The voltage between the electrodes is amplified and converted to a frequency-modulated signal. An optical coupler is used to isolate the fish from the cable and deck equipment. This is done to avoid or minimize interferences from high-level sources of noise on the very low-voltage circuits in the fish. For the same reason the dc power sent down the cable undergoes dc-dc conversion for use by the electronics. Temperature and pressure sensors are directly attached to pairs of wires on the tow cable.

<input checked="checked" type="checkbox"/>
<input type="checkbox"/>
<input type="checkbox"/>
<input type="checkbox"/>
PER LETTER



Dist	Avail and/or Special
A-1	

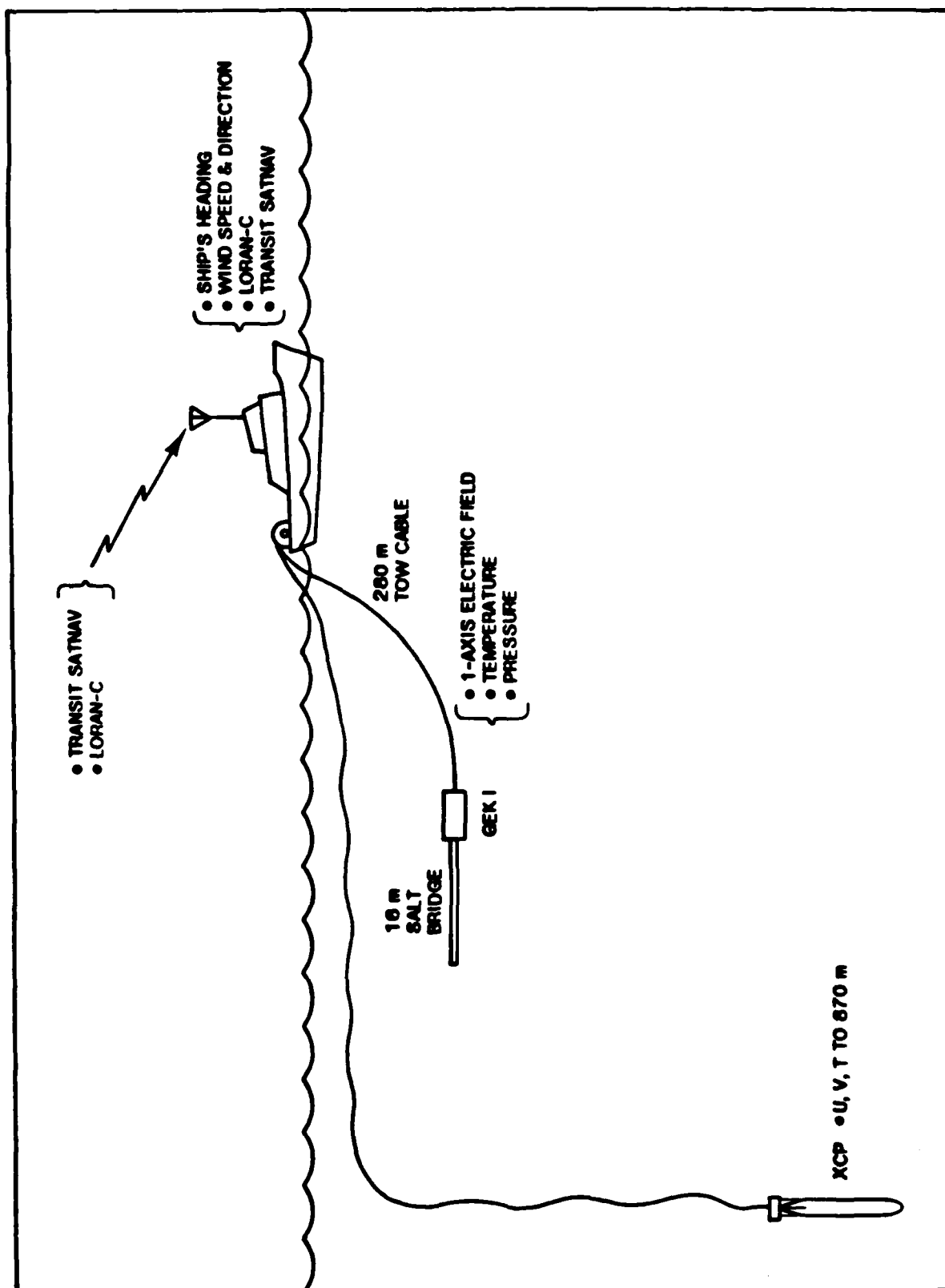


Figure 1: Depiction of the information and measurements gathered on the USNS Lynch cruise in December 1983.

BLOCK DIAGRAM OF GEK FISH AND CONTROL DECEMBER 1983

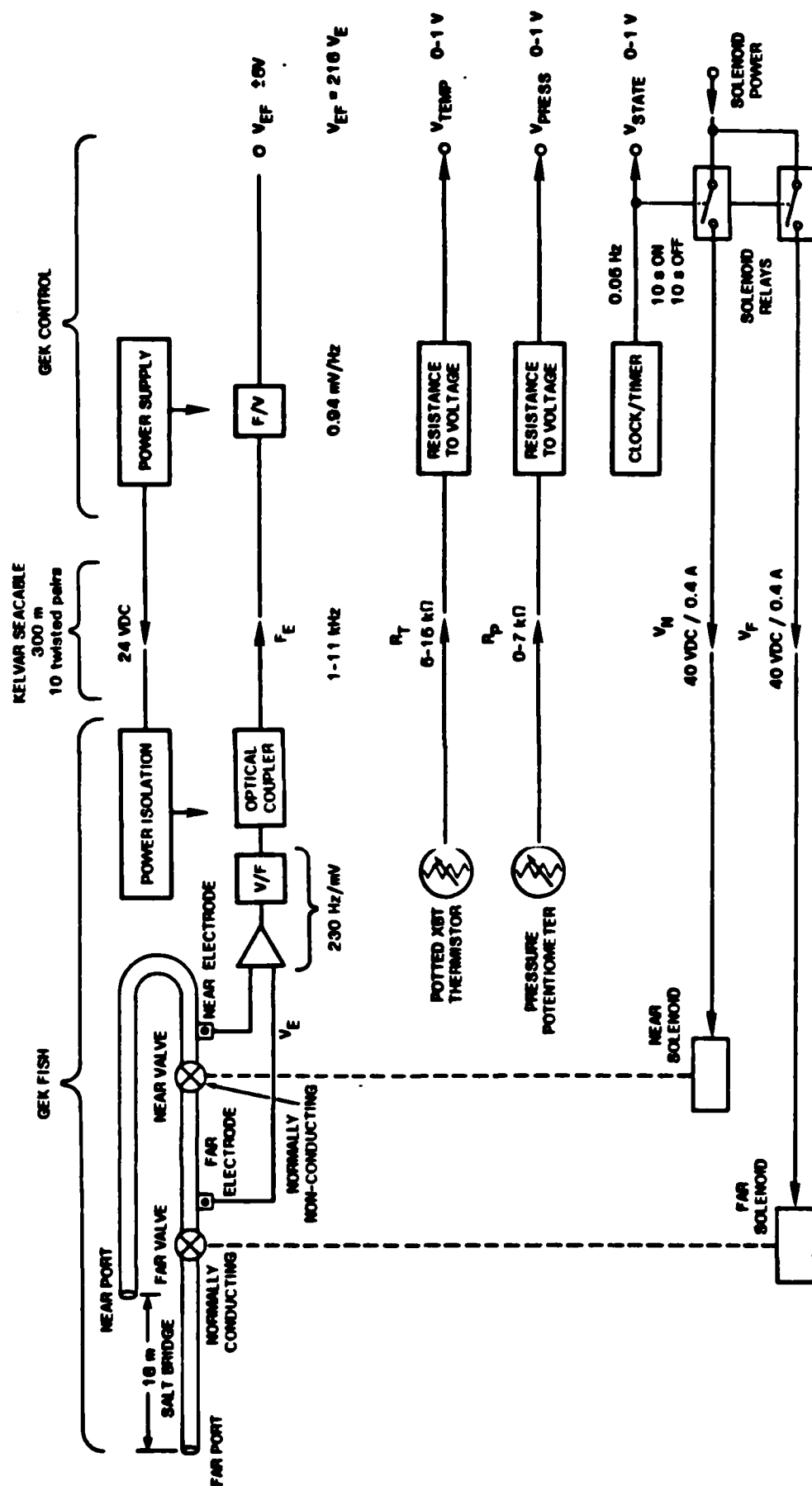


Figure 2: Block diagram of the GEK fish and controller.

The deck box or GEK controller sends dc power to the fish, receives analog voltages and frequency modulated signal and determines the resistances of the temperature and pressure sensors. An internal clock regulates the on/off sequences of the solenoid valves, and a frequency to voltage converter returns the electrode voltage to an analog value. Another diagram of the GEK system is presented in Fig. 3 where all important components of the system are depicted. The rubidium clock was used to provide a local time standard of accuracy sufficient to allow us to make range-range determinations using the LORAN-C receiver.

The processing of the data is diagrammed in Fig. 4. The input data consists of one-second values of the GEK voltages and LORAN ranges (or time differences) every 15-20 s. The output of the program on the HP9845T are 5-minute averages of the quantities in the lower right-hand box printed every minute. That is, all quantities were averages over 5 min., but the averaging window was slipped 1 min. at a time. Thus the display was 2.5-3.5 min behind real time.

A second data acquisition system was aboard to support the XCP part of the program. This gear is shown in Fig. 5 and is rather standard for our operations. Another conventional setup was the XBT equipment. A Mk 9 XBT deck box was borrowed from Sippican Ocean Systems, Inc. and used with an HP85 calculator borrowed from our lab.

3. The Field Operations and Preliminary Results

The plan for the Lynch cruise was to conduct several joint XCP and Pegasus stations, traverse the Florida Current on reciprocal courses several times, conduct an experiment to measure depth-averaged vorticity in the Current and survey a cold core ring in the Sargasso Sea. The

GEK SYSTEM DECEMBER 1983

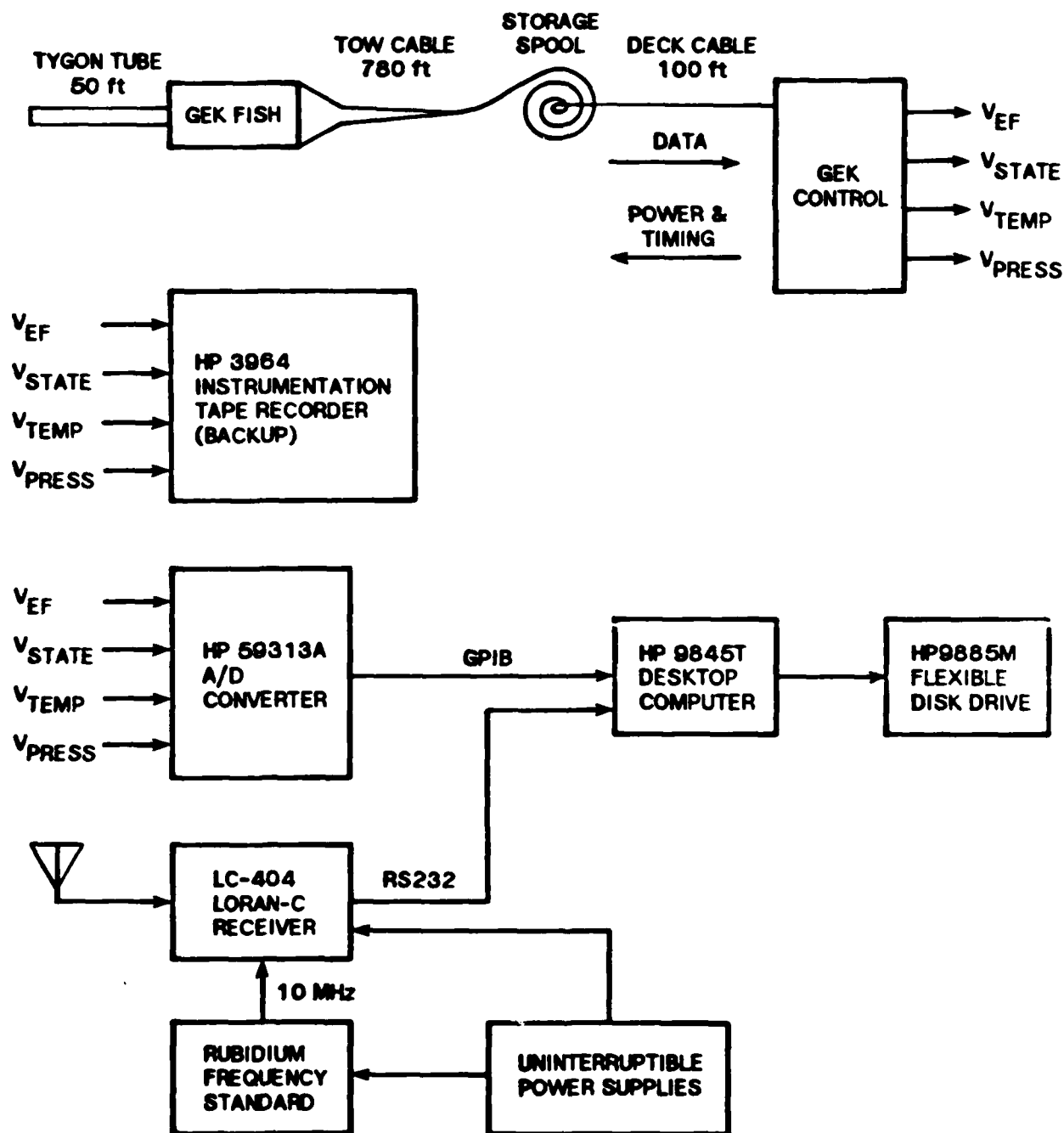


Figure 3: Description of GEK system; nomenclature, components and interconnections.

GEK ACQUISITION PROCESSING FLOW CHART **DECEMBER 1983**

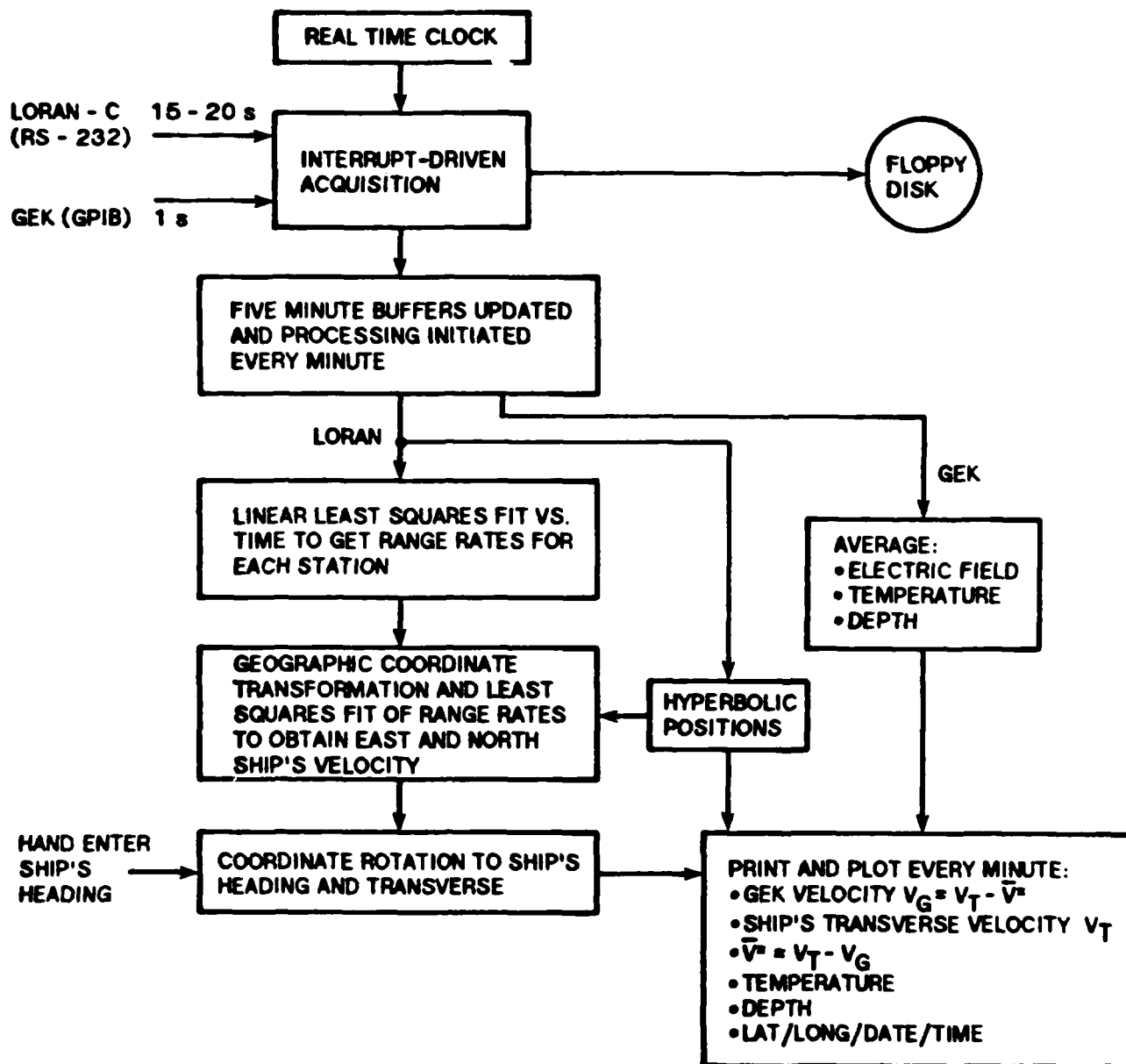


Figure 4: Data acquisition and processing flow chart.

XCP/CTD ACQUISITION SYSTEM
DECEMBER 1983
(ALSO USED FOR REPROCESSING GEK AND XBT DATA)

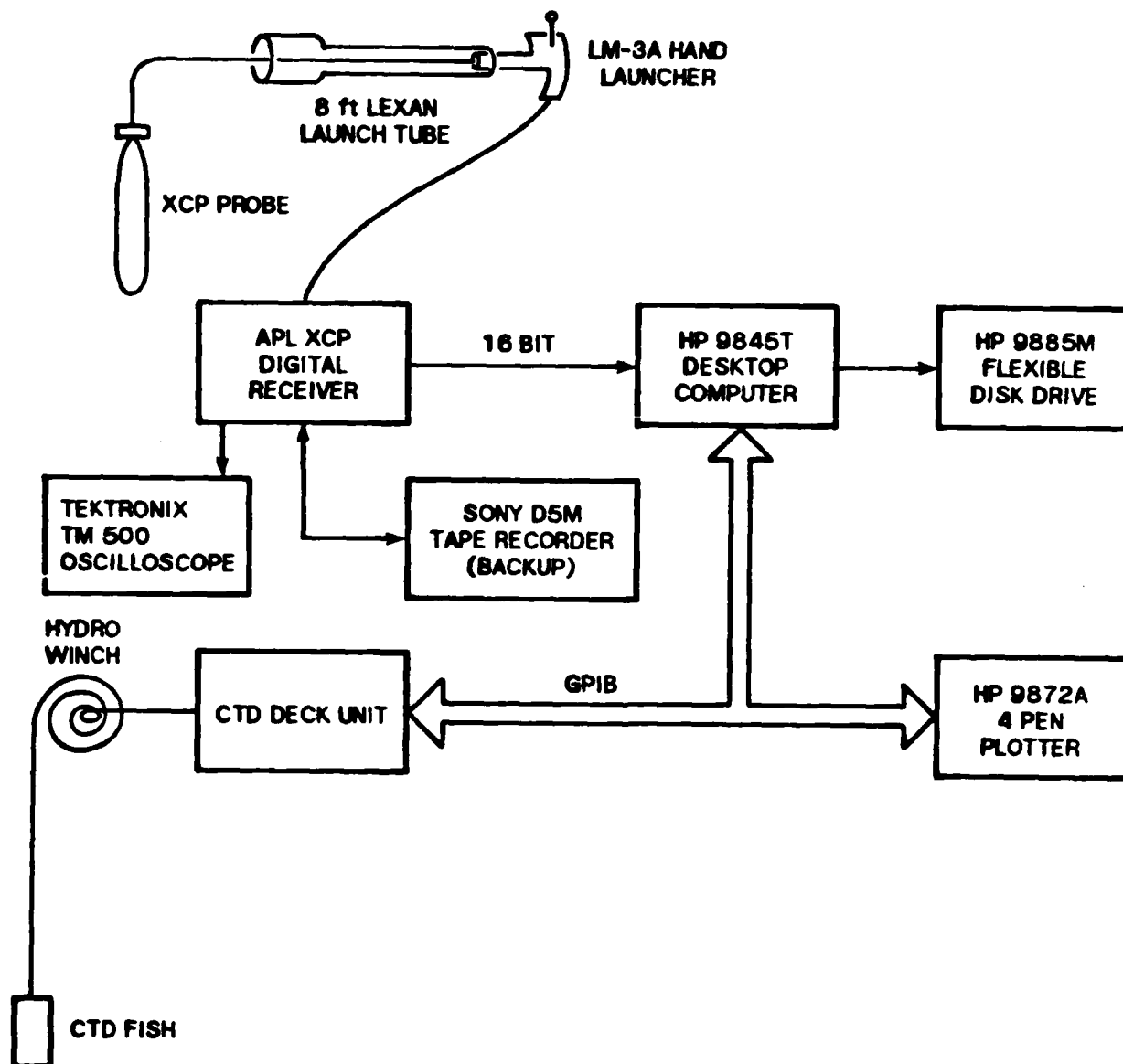


Figure 5: The XCP acquisition and processing system.

vessel track chart is presented in Fig. 6. The individual operations in the Florida Straits are hard to discern in this figure, so an enlargement of this area is shown in Fig. 7. Most of the cross-stream traverses occurred over the Jupiter Inlet to Settlement Point submarine cable, depicted by the wavy line. The star-like pattern near Memory Rock represents the experiment to determine barotropic vorticity on the anticyclonic side of the Current.

An example of the measurement of v and \vec{v}^* normal to the ship's heading is shown in Fig. 8. Analysis of these data and those from the other traverses is currently underway.

After about 5 days of operations we departed the Straits looking for a cyclonic or cold core ring. The purposes of this work were to obtain the first measurements of the barotropic structure of such a feature, to determine the baroclinic structure (in depth and horizontally) and to investigate the characteristics of inertial waves within and around a cyclonic ring. The ring was identified from satellite infrared images with the help of Peter Cornillon of URI and Jenifer Clark of the National Environmental Satellite Service. A cold core ring was found near Cape Hatteras based on the satellite information and XBTs. Figure 9 shows the contours of the depth of the 15 C isotherm in hundreds of meters. The ring was elongated and kidney-shaped, the 15 C isotherm rising from 600 to 250 m in the core. Figure 10 displays the velocity of the near-surface flow relative to the flow below 700 m from the velocity profiles. The velocity arrows also show the elongated structure. Maximum surface velocities were about 1 m/s.

The goals of the measurements were to test the wave-mean flow interaction theory of Kunze (1984) and to describe the baroclinic and

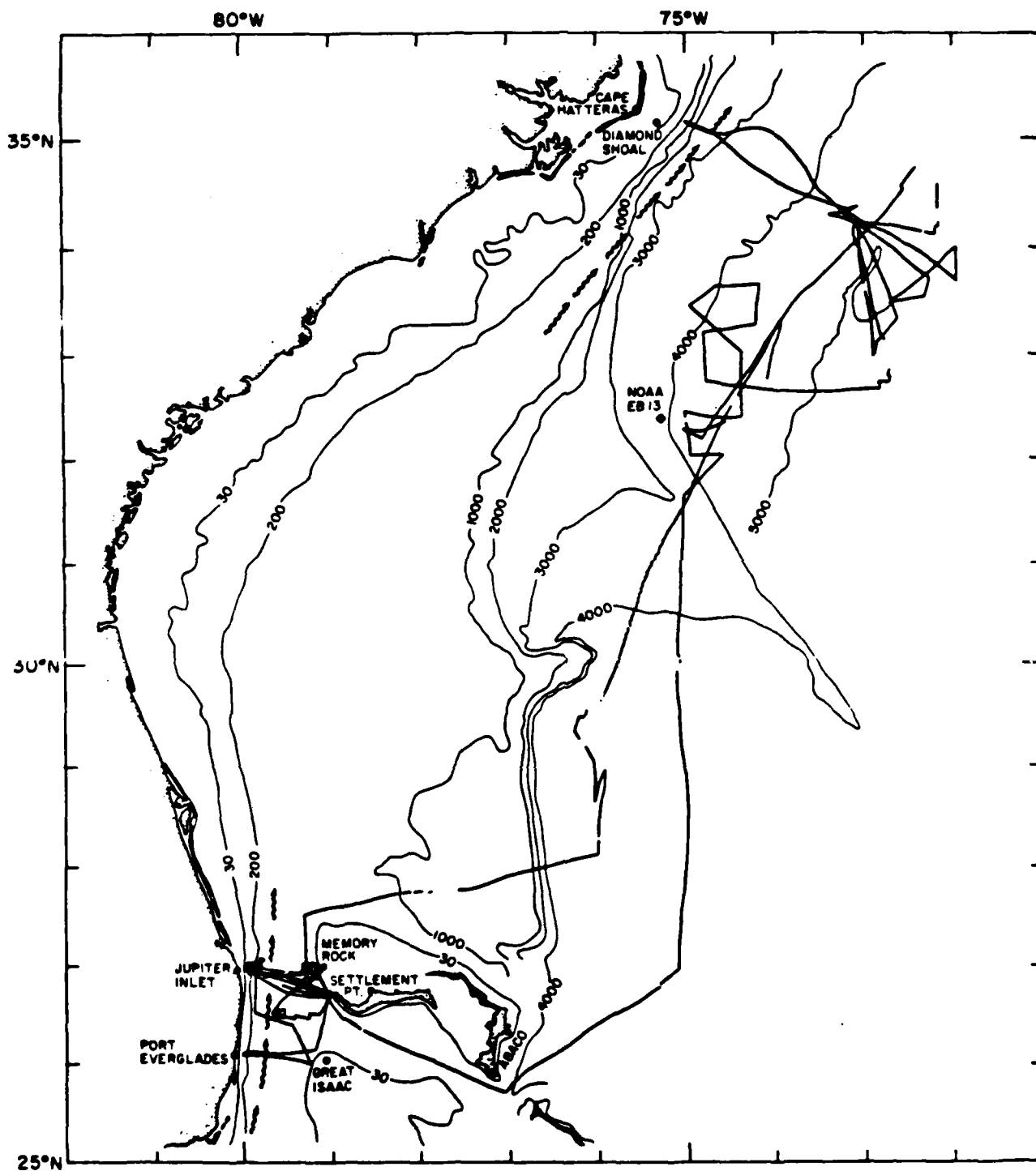


Figure 6: Vessel track chart for Lynch cruise, December 1983.

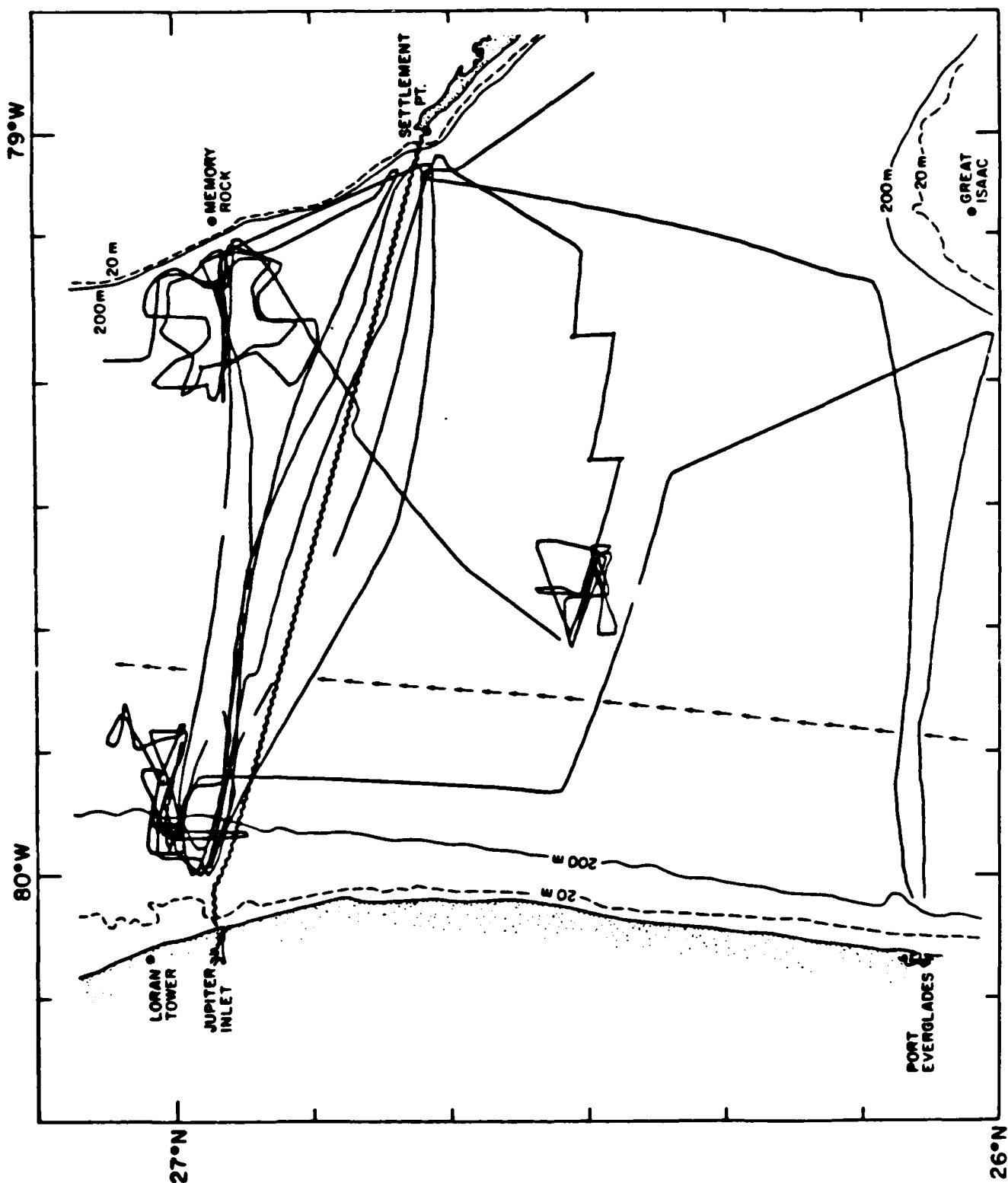


Figure 7: Lynch track chart for operations in the Florida Straits.

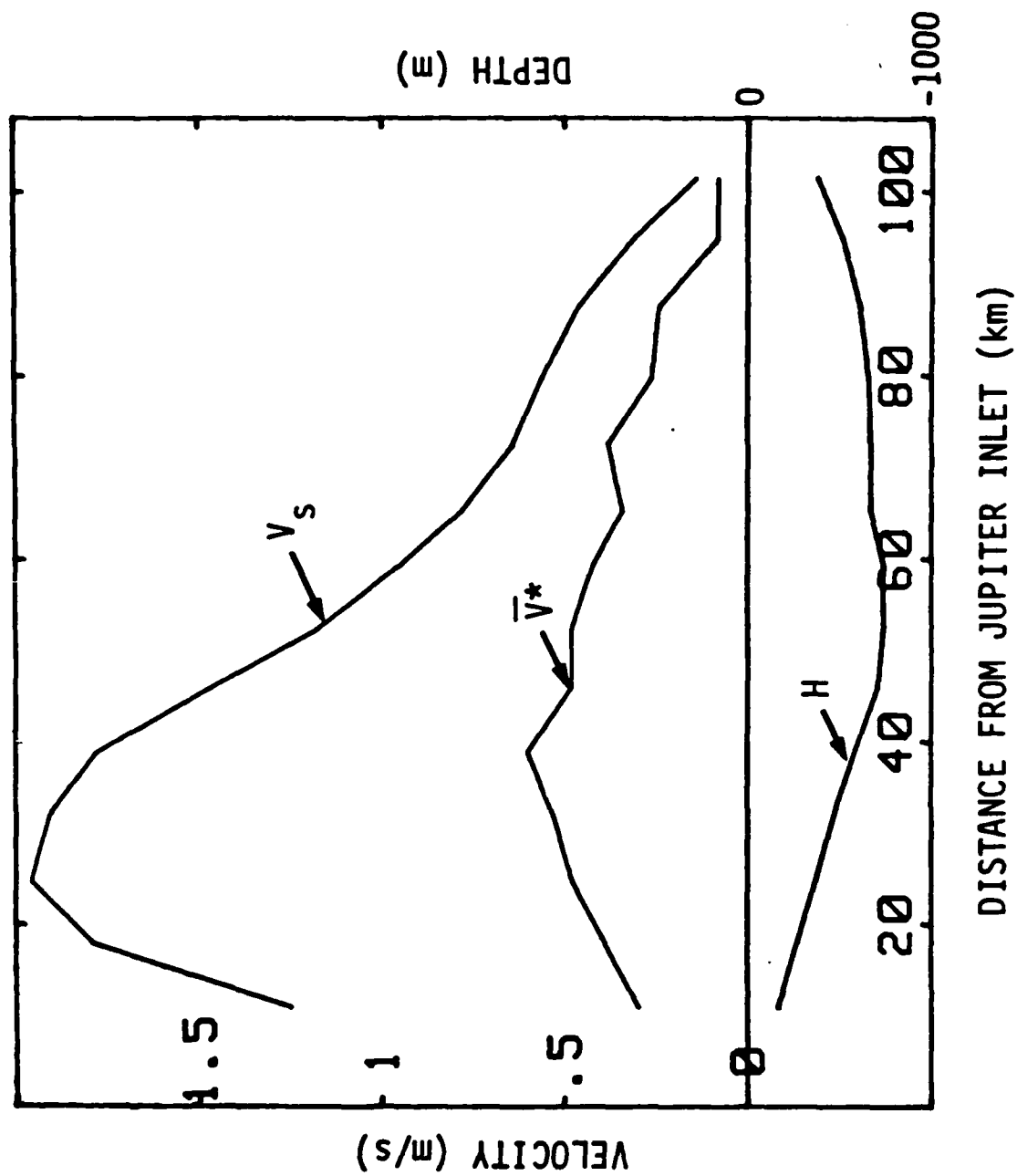


Figure 8: Surface (v_s) and depth averaged (\bar{v}) across the Straits from Florida to Grand Bahama Island.

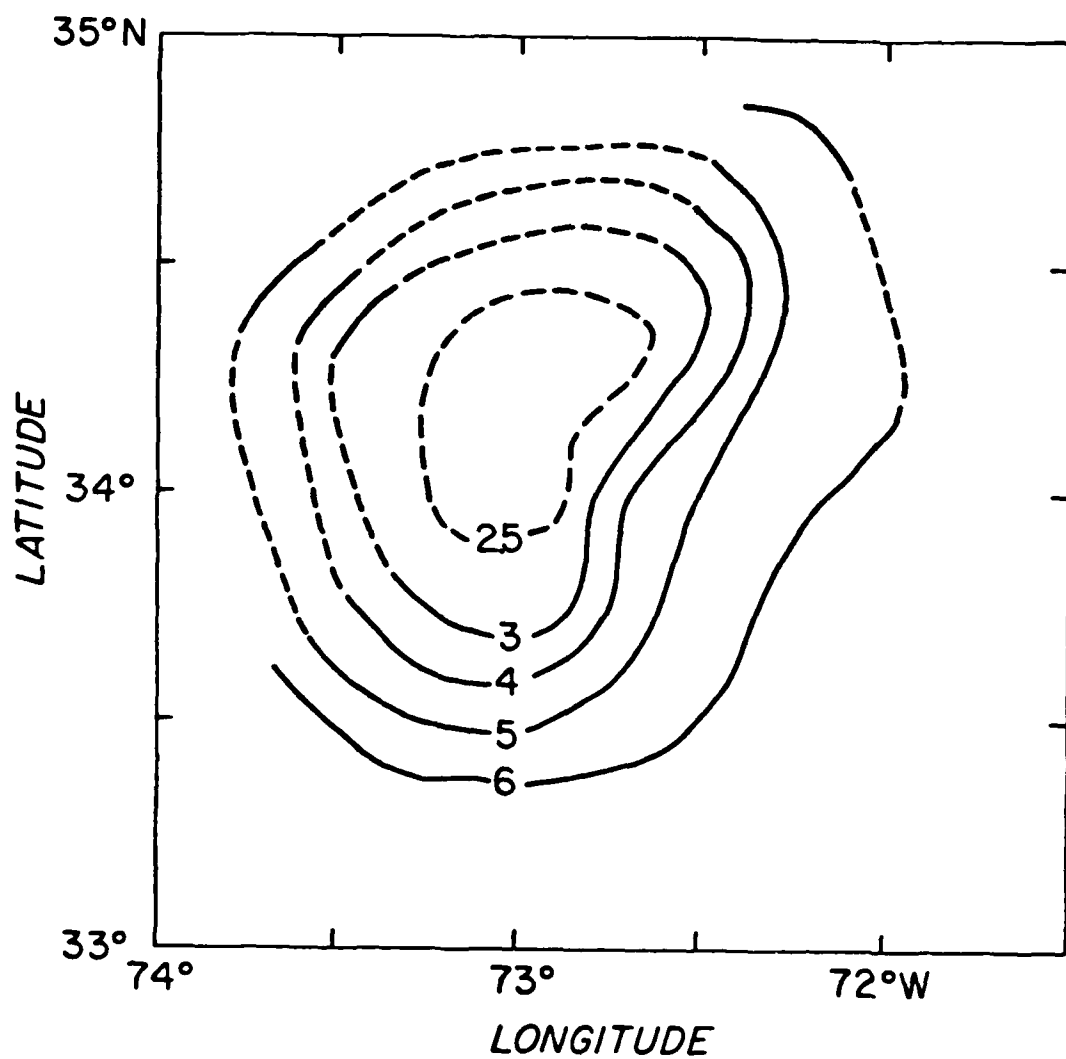


Figure 9: Depth of the 15 C isotherm in hundreds of meters in a cold-core ring found off Cape Hatteras in December, 1983. The cold dome rises 350 m above the background depth.

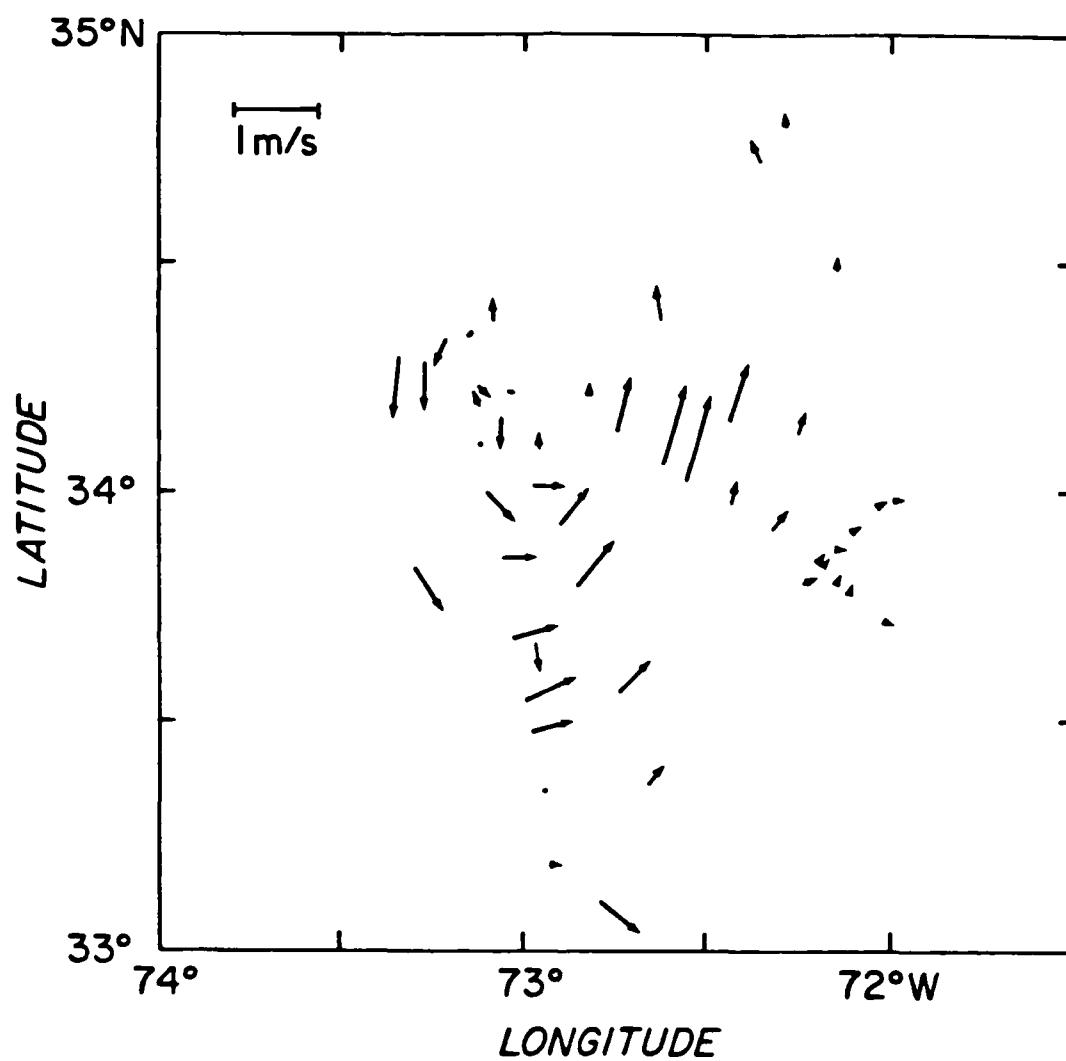


Figure 10: Surface velocities relative to 700-900 m from the velocity profiles. The arrows closely parallel the isotherm depth contours in Fig. 9.

barotropic structure of a cold-core ring from underway measurements. Using the techniques described above it was possible to discover and map the feature in terms of temperature and velocity. The velocity information is notable and the innovation of this particular research and cruise.

We set out to study the trapping and enhancement of near inertial motion within the region of negative vorticity. Kunze has shown that such waves undergo kinematic distortions in the presence of geostrophic shears and vorticity gradients. In particular, an inertial wave originating inside a region will not be able to escape that region, encountering turning points in the horizontal and critical layers in the vertical. This result has been experimentally borne out by measurements in the North Pacific Subtropical Front (Kunze and Sanford, 1984) where intense downward-propagating near-inertial waves were found on the warm, negative vorticity side of the front, and in a warm-core ring where an extremely energetic near-inertial wave was found at the base of the negative vorticity core. In a cold-core ring the negative vorticity region describes an annulus outside the high velocity region, and this is where we anticipated finding energetic downward-propagating near-inertial waves. While these waves were found, they were not as energetic as expected possibly because of calm weather prior to the experiment not being favorable for the generation of downward-propagating waves. It is also possible that the influence of advection and vertical shear (horizontal density-gradients) are more important to these waves in the outer annulus of a cold-core ring than they were in the front and the core of the warm-core ring. This will be resolved with further numerical experiments.

More interesting, an excess of upward-propagating near-inertial energy was found in the core of the ring. Figure 11 compares the clockwise-with-depth (CW), downward-propagating and anticlockwise-with-depth (ACW), upward-propagating energy-preserving spectra from profiles collected outside the core (upper frame) and in the core (lower frame). Outside the core, downward-propagating (CW) energy exceeds upward-propagating as is usually observed in the ocean. The only unusual feature of the clockwise spectra being that the peak is at very small wavelengths (30 m). Inside the core, upward-propagating (ACW) energy predominates. Upward-propagating near-inertial waves have been previously observed in the core of a cold-core ring by Richardson, Maillard and Sanford (1979). This suggests that such features are common to cold-core rings. We are confident that this unique data set will teach us much about the behavior of near-inertial waves in geostrophic shear.

The anticyclonic circulation to the barotropic component of the ring is clearly revealed in Fig. 12. It is remarkably strong. In fact, that is one point that came from this work: the barotropic flow is often quite strong (>0.5 kt). While we were conducting this work we determined that the surrounding or ambient water was moving to the WNW (290T) at 25 cm/s. This flow has been removed from the circulation pattern displayed in Fig. 12. That this background flow was real was confirmed by the fact that the ring was being flattened against the side of the Gulf Stream just to the west.

After conducting the ring survey, we set off to measure the transport of the Gulf Stream off Cape Hatteras. The weather was quite rough, but we were able to continue our program nonetheless due to the emphasis on expendables and towed sensors. The temperature section for

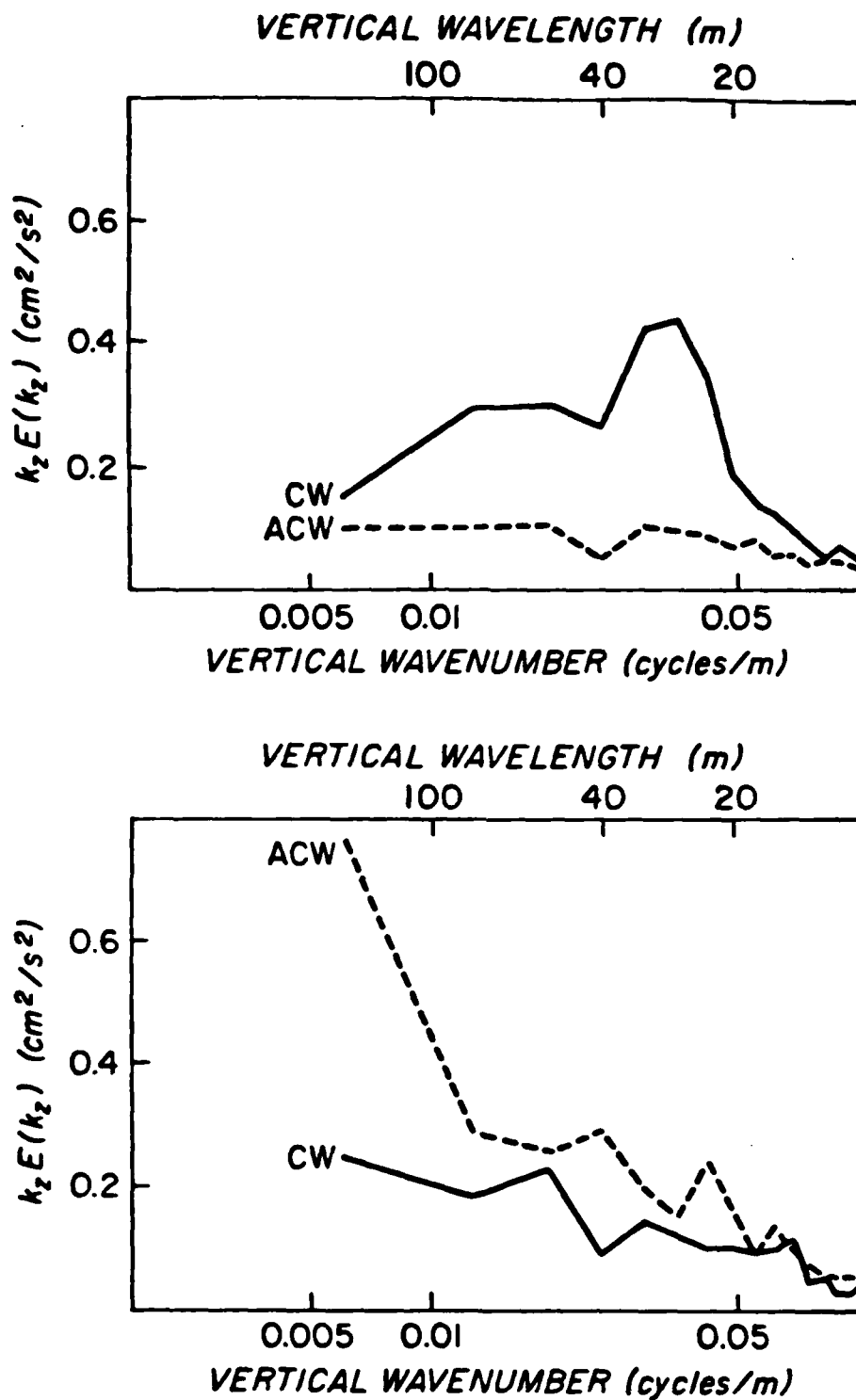


Figure 11: Energy-preserving clockwise-with-depth (solid) and anticlockwise-with-depth (dashed) spectra outside the cold core (upper frame) and within the core (lower frame). Clockwise-with-depth values correspond to downward-propagating near-inertial energy while anticlockwise-with-depth values correspond to upward-propagating energy. Outside the core the energy is dominantly downward-propagating as is usually found in the ocean. Within the core upward-propagating energy predominates.

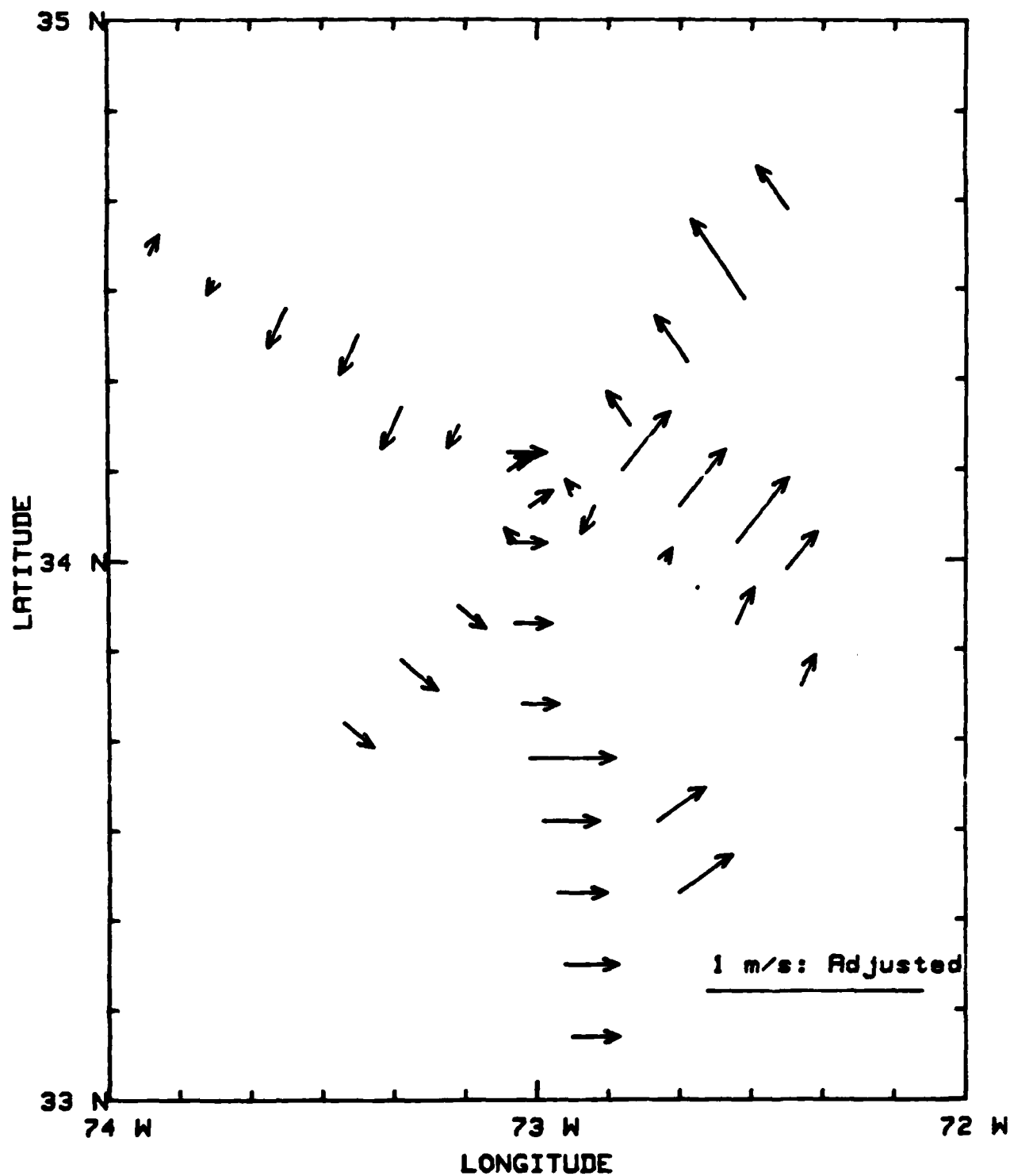


Figure 12: Barotropic velocity component normal to the vessel heading. The arrows are not true vectors, but represent the component pointing in the normal-to-track direction.

this leg is presented in Fig. 13. Note that the cold ring is right up against the Stream, not being more than 2 Rossby radii apart. This seems to be a limiting separation for a stable coexistence. The velocity data are presented in Fig. 14. These data have the expected structure; the transport maximum is offshore from the surface speed maximum; there is a strong counterflow on the shelf side. The volume transport is about 43 Sv in the Stream and -14 Sv in the counter flow. It is interesting that the sum is about 30 Sv, the average transport of the Florida Current. Is there no net transport gain to the Stream from Miami to Hatteras?

The new visibility of the barotropic flow component is long overdue. We have been operating in ignorance of the barotropic flow; it is little quantified in comparison to the baroclinic which can be described by BT and hydrodata. We are especially pleased with the ease in obtaining these data and the new insights that have come and will yet appear. This program was partially supported by NOAA under contract NAB1AAD-00078. This important support is gratefully acknowledged.

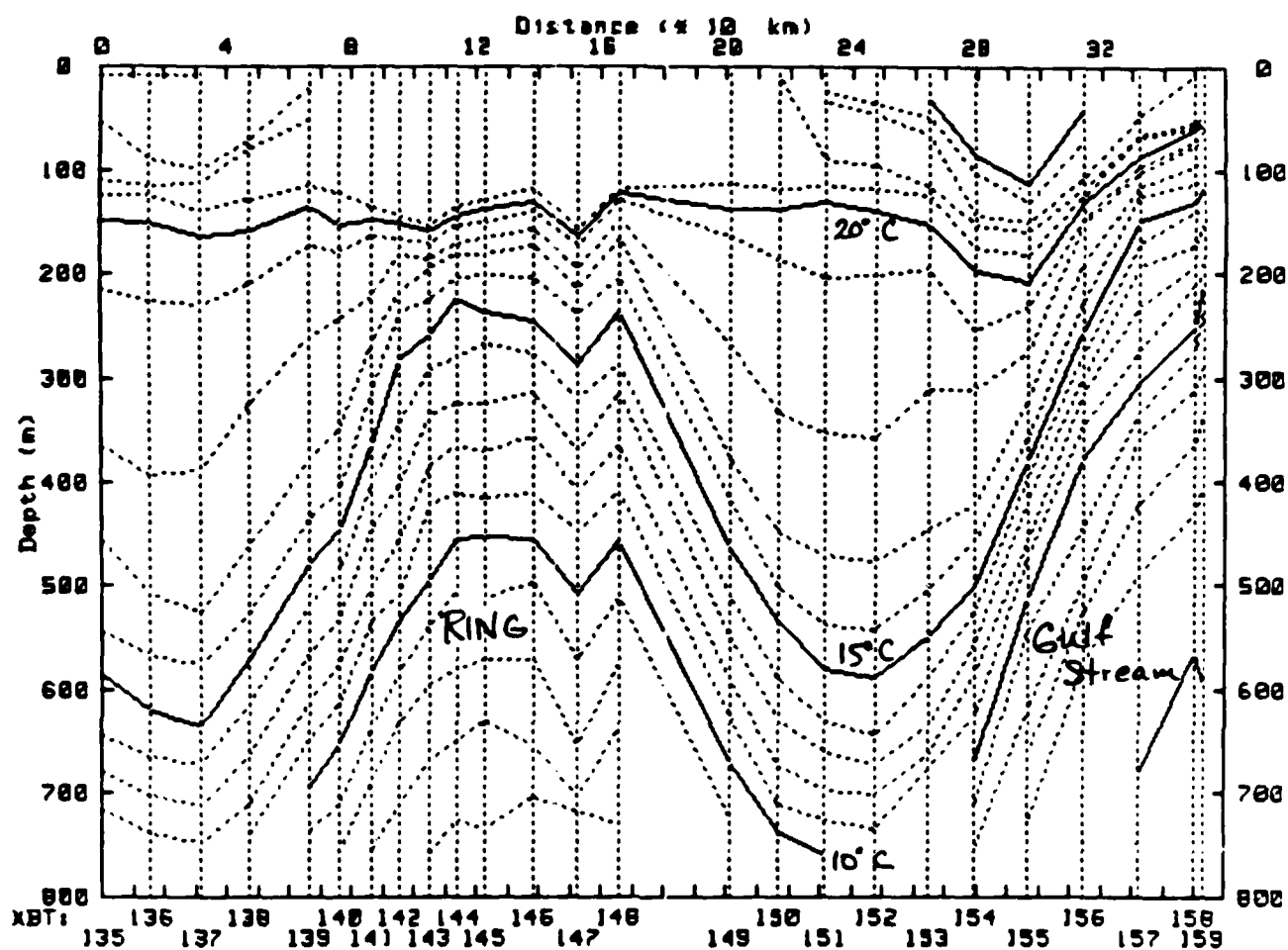


Figure 13: Temperature section from along a heading of about 300T from the SE side of the ring, across its center and on to Cape Hatteras.

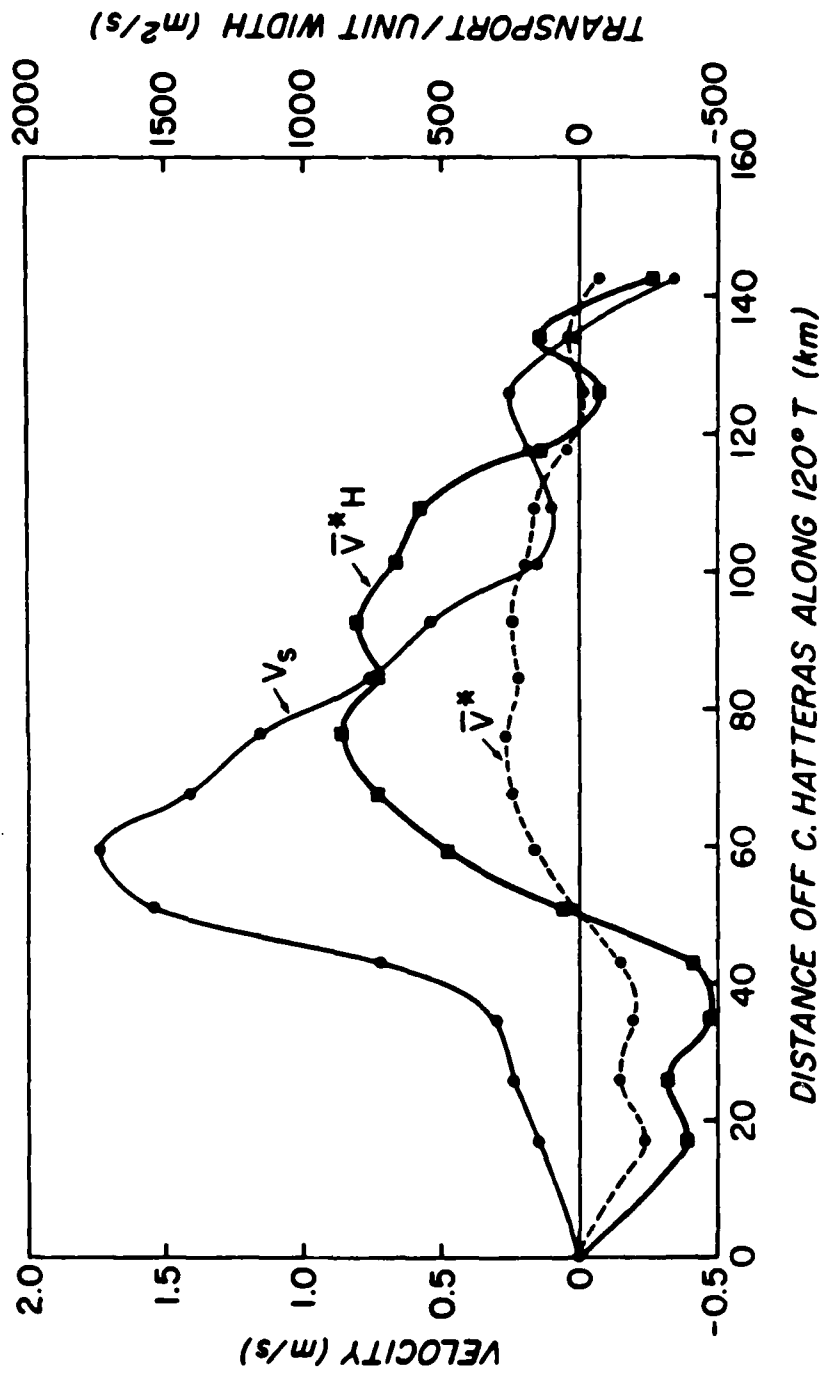


Figure 14: Velocity and transport observations across the Gulf Stream along the track of Figure 13.

References

Kunze, E., 1984:

Near-inertial wave propagation in geostrophic shear.

Kunze, E., and T. B. Sanford, 1984:

Observations of near-inertial waves in a front. Submitted to
J. Phys. Oceanogr.

Richardson, P. L., C. Maillard and T. B. Sanford, 1979:

The physical structure and life history of cyclonic Gulf Stream
ring Allen. J. Geophys. Res., 84, 7727-7741.

END

FILMED

2-85

DTIC

